Advances in Hollow Fiber Membranes Simulation for Multicomponent gas separation: Combining Physical Models and Neuro-Fuzzy Systems

Bryand J. Garcia-Sigales[1], Jose A. Ruz-Hernandez[1], Jose-Luis Rullan-Lara[1], Mario Antonio Ruz Canul[2], Alma Y. Alanis[2] and Juan Carlos Gonzalez Gomez[1]

[1]Facultad de Ingenieria, Universidad Autonoma del Carmen, Av. 56 # 4 x Av. Concordia, Col. Aviación, C.P. 24180, Cd. del Carmen, Campeche, México.
bgarcia@pampano.unacar.mx; jruz@pampano.unacar.mx; jrullan@pampano.unacar.mx; jcgonzalez@pampano.unacar.mx.
[2]Centro Universitario de Ciencias Exactas e Ingenierías, Universidad de Guadalajara, Blvd. Marcelino García, Barragan, Guadalajara 44430, Jalisco, México.
mario.ruz@academicos.udg.mx; alma.alanis@academicos.udg.mx;

Abstract. The separation of Natural Gas/CO_2 using hollow fiber membranes is essential for industrial applications, particularly in the oil and gas sector. Traditional modeling approaches, such as "black-box" models based on artificial neural networks (ANNs), offer high accuracy in parameter estimation but lack physical interpretability, making them unreliable for large-scale applications with variable operating conditions. Conversely, "white-box" models, grounded in physical laws and conservation principles, provide better scalability and physical insight but often require complex derivations and exhibit high uncertainty when experimental data is insufficient or when key parameters, such as gas permeability, must be inferred from empirical correlations.

To address these limitations, this study introduces a "gray-box" approach using an Adaptive Neuro-Fuzzy Inference System (ANFIS), which combines the data-driven adaptability of ANNs with the interpretability of fuzzy logic systems. The proposed white-box model is enhanced with ANFIS-based optimization to improve CO_2/CH_4 separation performance in hollow fiber membranes.

This study underscores the critical role of neuro-fuzzy systems in bridging physical modeling and machine learning, providing a robust and efficient approach for industrial gas separation. Integrating ANFIS with physical models enhances model reliability. It lays the foundation for scalable, real-world applications in the oil and gas industry, offering a more adaptive and data-efficient alternative to conventional approaches.

Keywords: Artificial Intelligence, Artificial Neural Networks, Adaptive Neuro-Fuzzy Inference System, Hollow Fiber Membranes, Gas Separation.

https://doi.org/10.61728/AE20255008

1 Introduction

Modeling membrane modules is a cornerstone for advancing gas separation technologies in industrial applications. By leveraging calculations and simulations, engineers can explore and optimize a wide range of configurations and operating parameters, enabling efficient systems to separate carbon dioxide (CO_2) from natural gas, which primarily consists of methane (CH_4) and other gases. These processes are particularly critical in the oil and gas industry, where their optimization directly impacts operational efficiency, cost-effectiveness, and environmental sustainability [1, 2].

Despite their importance, the separation of gases using membrane modules poses significant challenges that stem from the limitations of existing modeling approaches. In parallel, the oil and gas sector is undergoing a digital transformation driven by Industry 4.0, which integrates automation, data analysis, and modeling to meet operational and economic demands. This era, also known as the "age of intelligence", promotes the use of advanced technologies, such as artificial intelligence and machine learning, to improve resource management, reduce inefficiencies, and enable sustainable industrial practices [3]. Within this framework, membrane modeling plays a pivotal role in bridging simulation with strategic decision-making, establishing a foundation for developing advanced separation systems that align with the principles of sustainability and adaptability [2].

A key aspect of this transformation is incorporating intelligent systems in industrial applications, designed to mimic human cognitive processes. Inspired by biological structures, Artificial Neural Networks (ANNs) acquire knowledge through experience, allowing them to automate tasks and model nonlinear systems with significant complexity [4]. Introduced in 1959 by Frank Rosenblatt, the Perceptron was a milestone in neural computing, establishing the foundation for ANNs [5, 6]. Building on this foundation, modern approaches, such as the Adaptive Neuro-Fuzzy Inference System (ANFIS), combine the learning capabilities of ANNs with the rule-based interpretability of fuzzy logic systems. This hybrid architecture enables ANFIS to address imprecision and uncertainty while optimizing industrial processes, including separating CO_2 from natural gas in hollow fiber membranes [7, 8].

Traditional "black-box" models, such as ANNs, excel at approximating complex nonlinear relationships. These models are called "black-box" because they operate based on input and output data without revealing the internal workings of the system. However, their lack of physical interpretability limits their application in industrial settings where extrapolation beyond the training data is essential [8, 9]. This shortfall makes black-box models unreliable for large-scale applications or scenarios involving variable operating conditions.

On the other hand, "white-box" models, grounded in physical laws and conservation principles, provide interpretability and scalability, allowing for robust predictions in diverse industrial scenarios. Yet, these models often require intricate derivations and depend on precise parameter estimation, which can be challenging when key variables, such as gas permeability, cannot be measured directly and must be inferred from empirical correlations. This limitation introduces significant uncertainty, particularly in multicomponent systems like CO_2/Natural Gas separation [7, 10].

To address these challenges, "gray-box" models that combine the strengths of black-box and white-box approaches have emerged as a promising solution. Among these, neuro-fuzzy systems, such as ANFIS, stand out for their ability to integrate data-driven adaptability with physical interpretability. Recent applications of ANFIS in gas separation demonstrate its effectiveness in addressing uncertainty and nonlinearity [8]. More importantly, ANFIS's ability to dynamically adapt to varying operating conditions instills confidence in its suitability for industrial environments. It achieves a balance between accuracy and scalability, making it an ideal tool for process optimization and control in industrial environments [9].

This study proposes a white-box model enhanced with ANFIS for the separation of CO_2/Gas Natural in hollow fiber membranes. By integrating the physical foundation of white-box modeling with the adaptability of neuro-fuzzy systems, this approach overcomes the limitations of traditional modeling paradigms. The proposed framework aims to:

- Reduce parameter uncertainty by leveraging the strengths of physical models and ANFIS.
- Optimize membrane design to enhance separation efficiency.
- Provide scalable and robust solutions tailored to the operational demands of the oil and gas industry.

The integration of ANFIS with white-box models not only bridges the gap between interpretability and adaptability but also lays the groundwork for developing sustainable and efficient industrial gas separation processes [10].

2 Methodology

2.1 Mathematical modeling of hollow fiber membrane

This model aims to describe the behavior of the separation system through mathematical relationships that account for the gas properties and the membrane's characteristics. The most critical considerations in this model are described as follows:

- The membrane does not deform under the applied pressure.
- The gases involved are considered ideal in all phases of the process.
- The pressure drop on the permeate and retentate sides can be calculated using the Hagen-Poiseuille equation.
- The permeation of chemical species is considered constant.

The model is based on a set of differential equations that describe the variation of the component flow along the membrane. Equation (1) describes the rate of change of the molar flow of component i on the retentate side of the membrane in the flow direction. Equation (2) represents the rate of change of the molar flow of component i on the permeate side. Equation (3) details the pressure variation along the membrane on the retentate side, considering the dynamic viscosity of the mixture and the membrane geometry. Finally, Equation (4) describes the pressure variation on the permeate side [1, 11].

$$\frac{dv_i^R}{dz} = -Pm_i(p_i^R - p_i^P)D_o\pi N \tag{1}$$

$$\frac{du_i^P}{dz} = Pm_i(p_i^R - p_i^P)D_o\pi N \tag{2}$$

$$\frac{dP}{dz} = -\frac{192ND_O(D + ND_O)RT\mu_m}{\pi(D^2 - ND_o^2)^3 P}u \tag{3}$$

$$\frac{dp}{dz} = \frac{128RT\mu_m}{\pi D_i^2 Np}v \tag{4}$$

Where Pm_i is Permeation of component i $\frac{mol}{cm^2 \cdot atm \cdot min}$, p_i^R and p_i^P denote partial pressures of component in the retentate and permeate section, atm, α is an ideal separation factor or permselectivity, N is the number of tubes or fibers, i is component index, u is flow rate on the permeate side $(mol \cdot s)$ and v is flow rate on the retentate side $(mol \cdot s)$. The internal diameter is denoted by D (m), while D_i and D_o refer to the internal and external diameter of the hollow fiber membrane (m), R is Ideal gas constant, T is temperatura and μ_m is dynamic viscosity of the mixture $(\mathrm{Pa} \cdot s)$.

To solve the differential equations, the MATLAB function *ode15s* was used. This function employs an adaptive implicit method based on Backward Differentiation Formulas (BDF). This approach is particularly suitable for stiff systems, as it can handle rapid and slow variations in a stable and efficient manner. First, the model equations and initial conditions were defined (see Tables 1 and 2). Then, error tolerances and the integration interval were configured. This setup allowed for precise and stable numerical solutions for the system of interest.

Dynamic Determination of Viscosity

The viscosity of a pure fluid can be determined using the Chapman-Enskog solution, which is based on the Boltzmann transport equation. This approach assumes that molecular interactions can be approximated by those of Lennard-Jones particles with a potential function.

Table 1. Initial Conditions of the Process.

Parameter	Value	Unit
Initial Pressure in Retentate	29.607	atm
Initial Pressure in Permeate	1	atm
Temperature	298.15	K
Total Initial Flow Rate	1	mol/s
Inner Fiber Diameter	400	Å
Outer Fiber Diameter	1000	Å
Number of Fiber	99472	-
Module Diameter	1	m

Medi et al. [12] and Khalilpour et al. [13].

Table 2. Initial Conditions of Chemical Species

Parameter	Mole Fraction	Permeance (P_{mi}) $[10^{10} mol/(m^2 \cdot Pa \cdot s)]$
CH_4	0.6	3.72
CO_2	0.2	134
C_2H_6	0.15	1.02
C_3H_8	0.05	0.2

Medi et al. [12] and Khalilpour et al. [13].

The dynamic viscosity of a gas μ_i is calculated using the kinetic theory of gases, which relates this property to the temperature T, the molar mass M, the collision diameter σ, and the collision integral Ω_μ.

$$\mu_i = 2.669 \times 10^{-5} \frac{\sqrt{T \cdot M}}{\sigma^2 \cdot \Omega_\mu} \tag{5}$$

The reduced collision integral is calculated by considering the possible trajectories of particles during their approach. An empirical correlation relates Ω_μ to temperatura.

$$\Omega_\mu = \frac{1.16145}{T^{*-0.14874}} + \frac{0.52487}{exp(0.77320T^*)} + \frac{2.16178}{exp(2.43787T^*)} \tag{6}$$

The viscosity of a diluted gas is related to the mole fraction x_i and the viscosity of the diluted gas component i, following Wilke's equation.

$$\mu_{mix} = \sum_i \frac{x_i \mu_i}{\sum_j x_j \varphi_{ij}} \tag{7}$$

The binary weighting factor φ_{ij} expressed as a function of the gas viscosity and the molecular weight of the component as follows.

$$\varphi_{ij} = \frac{\left[1 + \left(\frac{\mu_i}{\mu_j}\right)^{0.5} \left(\frac{M_i}{M_j}\right)^{0.25}\right]^2}{\left[8\left(1 + {M_i}/{M_j}\right)\right]^{0.5}} \tag{8}$$

Sensitivity Analysis in Permeation

Permeation is one of the most relevant parameters in membrane separation, as it determines the process's permeability and selectivity. Previous studies indicate that when the CO_2 concentration in the feed is below 20%, and the pressure is below 14.8 atm, the plasticization effect becomes negligible. For this reason, these values are often assumed to remain constant [14].

Although this work does not develop an explicit model for permeability variation a simulations were carried out in which the permeation of CH_4 was modified. This approach accounts for the fact that operating conditions—at least in wells located in the "Golfo de México"—exceed the referenced pressures, and these changes can influence the final gas volume required. This provides insight into the process sensitivity to potential variations in permeation.

2.2 Statistical Method

Correlation analysis is one of the most commonly used and reported statistical methods in scientific and medical research. Its visual representation is known as a scatter plot. It is used to confirm or refute the existence of a relationship between two variables based on the Pearson correlation coefficient described in Equation (9), [15].

$$\rho(a, b) = \frac{E(ab)}{\sigma_a \sigma_b} \tag{9}$$

Where $E(ab)$ represents the cross-correlation between a and b, and where $\sigma_a^2 = E(a^2)$ and $\sigma_b^2 = E(b^2)$ correspond to the variances of the variables.

When considering variables a and b, a scatter plot is a powerful tool that visually represents their ordered pairs within a coordinate system. It's not just a graph but a visual representation of the relationship between the two variables. When most points align closely with a straight line, the correlation is classified as linear. Conversely, the correlation is considered nonlinear if the points follow a curved pattern. However, if no discernible pattern is observed among the ordered pairs, it indicates the absence of a relationship between the two variables. To depict the curve or regression line that best fits the distribution of the ordered pairs, Equation (10) is applied.

$$y = a_0 + a_1 x_1 + a_2 x_2 + \cdots + a_m x_m \tag{10}$$

The correlation coefficient, or R, is a fundamental measure for assessing relationships between variables within a system. In the context of gas volume prediction, it helps us understand how changes in one variable, such as pressure or permeation, might affect the volume of separated gas in a hollow fiber membrane. The magnitude and direction of the correlation coefficient can be either positive (from 0 to 1) or negative (from -1 to 0). A value of R close to ±1 indicates a stronger correlation.

The determination coefficient R^2 is a crucial factor in predicting the volume of separated gas in hollow fiber membranes. It indicates the percentage of variability in the dependent variable that the independent variables can explain. This correlation analysis is instrumental in selecting representative variables for the ANFIS model, a process that significantly reduces model dimensionality and enhances predictive performance. The importance of this proper variable selection cannot be overstated, as it ensures the reliability and accuracy of our research.

To minimize model error, our study employs Gradient Descent Optimization (GDO) using the Least Squares Regression (LSR) method, as described in [15]. This strategic use of GDO allows us to identify the most influential variables in gas volume prediction, ensuring that only the most relevant variables are incorporated into the ANFIS model. This approach minimizes error and enhances our model's precision, providing a deeper understanding of the gas volume prediction process.

In addition to GDO, we calculated the Mean Absolute Error (MAE) and the Mean Absolute Percentage Error (MAPE) to evaluate the model's performance, following the methodology outlined in [15]. These error metrics help us assess the accuracy and reliability of our predictions. The rigorous validation of the model's performance ensures that our research is reliable and instills confidence in the accuracy of our predictions.

$$x = \begin{bmatrix} x_{11} & x_{12} & x_{13} & \cdots & x_{1k} \\ x_{21} & x_{22} & x_{23} & \cdots & x_{2k} \\ x_{31} & x_{32} & x_{33} & \cdots & x_{3k} \\ \vdots & \vdots & \vdots & & \vdots \\ x_{n1} & x_{n2} & x_{n3} & \cdots & x_{nk} \end{bmatrix} \quad y = \begin{bmatrix} y_1 \\ y_2 \\ \vdots \\ y_n \end{bmatrix} \tag{11}$$

The matrix "x" and the vector "y" from Equation (11) are shown in Equation (12).

$$\begin{gathered} x = [v_i^R \quad Pm_i \quad \mu_m \quad P] \\ y = [v_i^R] \end{gathered} \tag{12}$$

Therefore, we can denote $\boldsymbol{x_1}$ as $\boldsymbol{v_i^R}$, which in this case refers to the volume fo CH_4, $\boldsymbol{x_2}$ as $\boldsymbol{Pm_i}$ representing the permeance in the retentate, $\boldsymbol{x_3}$ as the viscosity in the permeate $\boldsymbol{\mu_m}$ and $\boldsymbol{x_4}$ a $\boldsymbol{P}$, which corresponds to the pressure in the permeate.

2.3 Intelligent Modeling with ANFIS

The technique to be implemented is an ANFIS, which combines two intelligent techniques, ANNs, and fuzzy logic, to leverage their strengths and overcome each technique's weaknesses. Layer 2 consists of round nodes or fixed operations. Equation 1 represents the output obtained between each pair of membership functions, where $\dot{\mu}$ is the membership function, A_i is the linguistic label, and w_i is the output or firing strength of each fuzzy rule [16 and 17].

$$w_i = \dot{\mu}_{A_i}(x_1) \times \dot{\mu}_{B_i}, \quad i = 1,2. \tag{13}$$

Layer 3 consists of normalizing the firing strengths. Layer 4 involves specific parameters known as "consequents," which allow for "defuzzification" to generate results within the original output range. Finally, Layer 5 concludes with an average of all outputs from Layer 4 to determine a single output result, as described by Equation E.C., where f_i corresponds to the combination of input values with the consequent parameters from Layer 4.

$$Total\ Ouput = \frac{\sum_i w_i f_i}{\sum_i w_i} \tag{14}$$

The neural network component allows the weights and parameters to be continuously adjusted through the learning process. The learning or training used in this work is called hybrid, as it combines least squares to estimate the output from one layer to the subsequent and gradient descent to propagate the error from one layer back to the previous one, minimizing it by adjusting the parameters.

For gradient descent, Equation E.C. shows the so-called cost function, described by the difference between the estimated and actual values, also known as the error E_p between the two signals. Gradient descent involves partial derivatives concerning α (a generic system parameter), as demonstrated in Equation E.C., which is based on Equation 5, applying the learning rate represented by η.

$$Total\ Ouput = \frac{\sum_i w_i f_i}{\sum_i w_i} \tag{15}$$

$$\frac{\partial E_p}{\partial \alpha} = \sum_{m=1}^{L} \frac{\partial E_p}{\partial \alpha} \tag{16}$$

$$\Delta\alpha = -\eta \frac{\partial E_p}{\partial \alpha} \tag{17}$$

Selection of Input Variables

To determine the best model configuration, three options for input data delays were evaluated:

Case 1

$$\hat{v}_i^R(k) = f\left[v_i^R(k-1) \quad Pm_i(k-1) \quad \mu_m(k-1) \quad P(k-1)\right] \tag{17}$$

Case 2

$$\hat{v}_i^R(k) = f\left[v_i^R(k-2) \quad Pm_i(k-2) \quad \mu_m(k-2) \quad P(k-2)\right] \tag{18}$$

Case 3

$$\hat{v}_i^R(k) = f\left[v_i^R(k-3) \quad Pm_i(k-3) \quad \mu_m(k-3) \quad P(k-3)\right] \tag{19}$$

The data were generated by the white-box model and subsequently loaded for analysis. The selection of input variables was guided by the methodology described previously, particularly correlation analysis.

3 Results and Discussion

3.1 Validation of Mathematical modeling of hollow fiber membrane

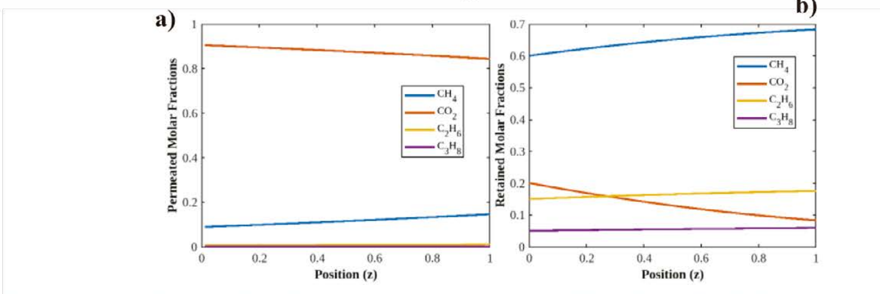

Fig. 1. a) Molar flow profiles of the retentate for four species (CH_4, CO_2, C_2H_6, C_3H_8) along the hollow fiber. b) Molar flow profiles of the permeate, showing the distribution of the same species in the permeate stream. The x-axis represents the axial length of the membrane, from the inlet to the outlet of the module.

In Figure 1(a), it can be observed that as the gas advances through the membrane module, the fraction of CH_4 in the retentate gradually increases, while the CO_2 fraction decreases steadily. This behavior aligns with the membrane's higher affinity for carbon dioxide, which tends to permeate more easily into the low-pressure stream. Consequently, CH_4 becomes "enriched" on the retentate side.

In Figure 1(b), the permeate stream initially exhibits a very high CO_2 content, confirming its high permeability. However, methane is not completely absent in the permeate but slightly increases along the module. This relative increase in CH_4 suggests that while CO_2 is the dominant species, the driving force (pressure and concentration gradients) allows some methane to pass through the membrane, particularly during the initial stages of the process or when the CO_2 concentration decreases.

For C_2H_6 and C_3H_8, their fractions in both streams are significantly lower than those of CH_4 and CO_2. Nevertheless, the observed trend aligns with the lower permeability of heavier hydrocarbons, maintaining slightly higher concentrations in the retentate.

These results highlight the importance of membrane selectivity and the driving force in the separation efficiency. The reduction of CO_2 in the retentate and its majority presence in the permeate suggest that the process is well-suited for applications aimed at CO_2 removal. On the other hand, the residual presence of CH_4 in the permeate indicates the need to optimize operational variables (e.g., operating pressure, module length, or feed velocity) to minimize methane losses and maximize the purity of the retentate gas. This model has been validated according to bibliographical data [12, 13].

Accordingo to Fig 2, the sensitivity analysis studied volumetric flow instead of molar flow to provide a more practical perspective for designing membrane separation processes. Increasing the permeance of a component significantly raises the partial volume of that component in the permeate. This phenomenon is particularly noticeable with methane (CH_4), whose partial volume increases substantially as CH_4 permeance rises. On the other hand, the presence of CO_2 and the hydrocarbons C_2H_6 and C_3H_8 may show more moderate variations, also depending on their respective permeances and affinities with the membrane. The combined effect of these changes is reflected in the final composition of the streams, highlighting that permeance is a key parameter for optimizing both the recovery and selectivity of each component.

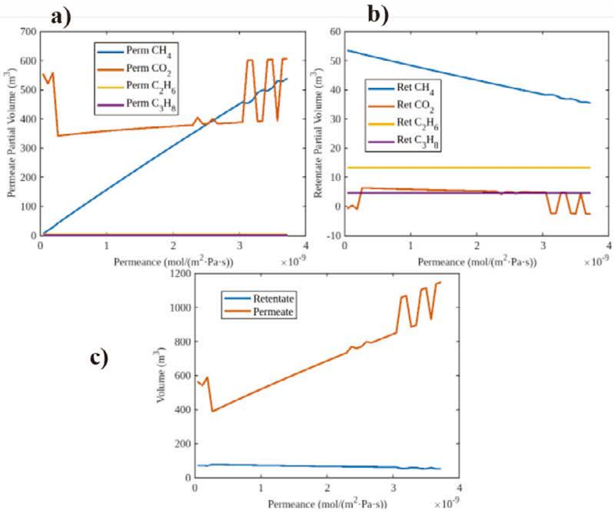

Fig. 2. Influence of CH_4 permeance on partial and total volumes in the permeate and retentate streams. a) Partial volumes of CH_4, CO_2, C_2H_6, and C_3H_8 in the permeate. b) Partial volumes of CH_4, CO_2, C_2H_6, and C_3H_8 in the retentate. c) Total volumes of the permeate and retentate as a function of permeance.

3.2 Results Statistical Method

This section presents and analyzes the results obtained from the multiple linear regression model and the corresponding evaluation metrics. The results are summarized in Tables 3, 4, and Fig. 3, which detail the model parameters and performance metrics. These results were obtained to predict the volume of gas separated in a hollow fiber membrane.

The proximity of the points to the diagonal line strongly indicates the model's ability to predict dependent variable values with exceptional accuracy. This is further reinforced by the quantitative results in Tables 3 and 4, where a coefficient of determination (R^2) is close to 1, and minimal errors (MAE and MAPE) are observed. The graph also allows for identifying potential outliers or regions where the model could improve its accuracy, providing a comprehensive view of the model's performance.

The intercept a_0 is extremely close to zero, suggesting that, within the context of the model, the value of the dependent variable y is practically null when all independent variables (x_1, x_2, x_3, x_4) are zero. This result is consistent with the normalization applied to the data during the modeling process. The negative coefficients of a_1, a_2, and a_3 indicate an inverse relationship between the independent and dependent variables.

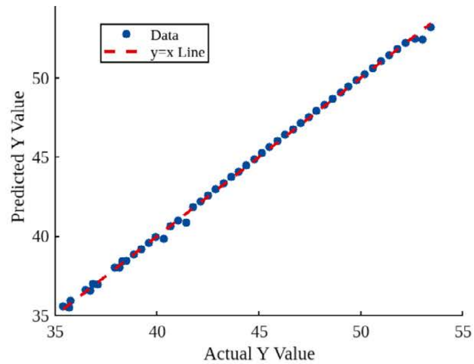

Fig. 3. Actual vs. predicted values of "y" for a multiple linear regression model. The blue dots represent the actual data points, while the red dashed line represents the ideal.

$$y = 1.606e^{-12} - 0.6610x_1 - 0.4351x_2 - 02000x_3 \tag{12}$$

Table 3. The values of a_k

Parameter	MCS
a_0	$1.606e^{-12}$
a_1	-0.6610
a_2	-0.4351
a_3	-02000

The coefficient of determination R^2 of 0.9990 indicates that the model explains 99.90% of the variability in the dependent variable, suggesting an almost perfect fit to the data. This high R^2 value is supported by the model's predictions, which have minimal error in absolute and percentage terms, with low MAE (0.1180) and MAPE (0.27%) values. These results demonstrate the model's precision and trustworthiness in predicting the volume of gas separated in the hollow fiber.

Table 4. Comparison of Regression Model Performance Metrics.

Metric	Value
R^2	0.9990
MAE	0.1180
MAPE	0.27%

3.3 Results of Intelligent Modeling with ANFIS

Integrating the ANFIS with the white-box model significantly improved predictive accuracy and adaptability. Figures 4, 5, and 6 illustrate the training performance of the

ANFIS for Cases 1, 2, and 3, respectively, highlighting the evolution of error metrics, step size adjustments, and the alignment between predicted and actual outputs.

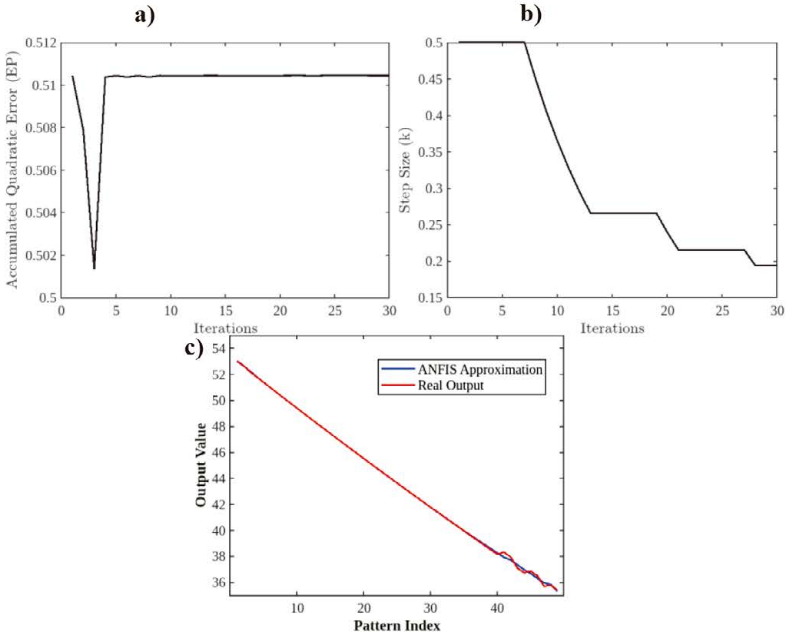

Fig. 4. Evolution of error and step size during the ANFIS training process and comparison between the approximated and real output. a) Accumulated Quadratic Error (EP) as a function of iterations. b) Step size α_k as a function of iterations. c) Comparison between the approximated output obtained by ANFIS and the real output. The results correspond to Case 1.

In Figure 4(a), the Accumulated Quadratic Error (EP) for Case 1 decreases sharply within the first 50 iterations, followed by a gradual stabilization. This rapid reduction indicates effective learning during the initial training phase, while the plateau suggests convergence toward an optimal solution. A similar trend is observed in Figures 5(a) and 7(a) for Cases 2 and 3. However, Case 3 exhibits a marginally slower convergence rate, likely due to the increased complexity introduced by delayed input variables. The final EP values for all cases remain below 1×10^{-3}, demonstrating the model's capability to minimize prediction errors effectively.

The step size (α_k), depicted in Figures 4(b), 5(b), and 6(b), reflects the adaptive nature of the hybrid learning algorithm. Initially, larger step sizes facilitate rapid parameter adjustments, accelerating error minimization. As training progresses, the step size decreases, ensuring finer tuning of the ANFIS parameters to avoid overshooting local minima. Case 3 (Figure 6(b)) maintains a slightly higher step size throughout training, which may enhance exploration in a more complex input space. This adaptability underscores ANFIS's robustness in balancing exploration and exploitation during optimization.

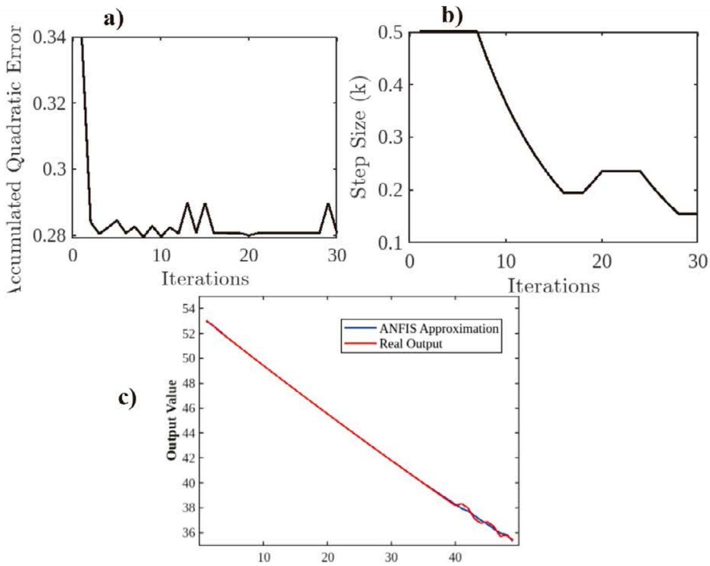

Fig. 5. Evolution of error and step size during the ANFIS training process and comparison between the approximated and real output. a) Accumulated Quadratic Error (EP) as a function of iterations. b) Step size α_k as a function of iterations. c) Comparison between the approximated output obtained by ANFIS and the real output. The results correspond to Case 2.

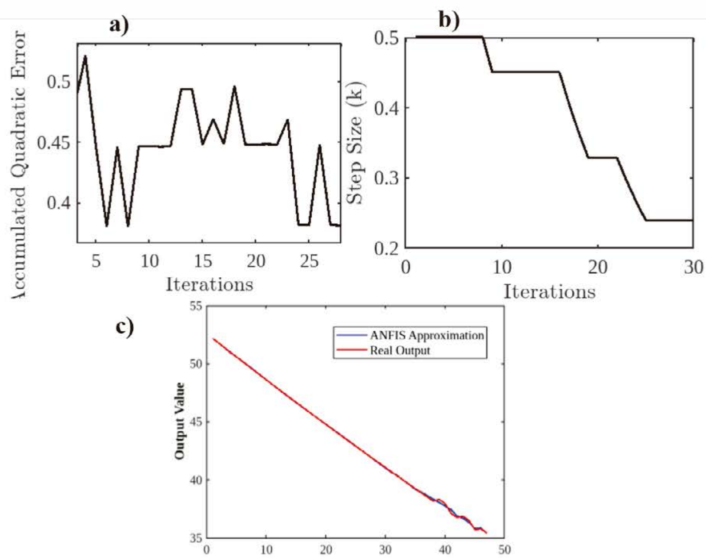

Fig. 6. Evolution of error and step size during the ANFIS training process and comparison between the approximated and real output. a) Accumulated Quadratic Error (EP) as a function of iterations. b) Step size α_k as a function of iterations. c) Comparison between the approximated output obtained by ANFIS and the real output. The results correspond to Case 3.

4 Conclusion

This study introduces a hybrid "gray-box" model combining physico-mathematical frameworks and neuro-fuzzy systems (ANFIS) to optimize hollow fiber membranes for multicomponent gas separation. The integration balances accuracy, interpretability, and adaptability, achieving exceptional predictive performance (R^2 = 0.9990, MAE = 0.1180). Sensitivity analysis confirmed permeance's pivotal role in selectivity, especially under varying CO_2/Gas Natural ratios. ANFIS enabled dynamic adaptation to complex scenarios, ensuring robustness in real-world environments.

To advance the model, future research will focus on three axes: improving physical models, enhancing ANFIS, and integrating control systems. Physical model refinements include iterative subroutines for gas solubility/diffusivity (addressing non-ideal effects like plasticization), turbulent flow pressure-drop equations for high-pressure operations, and cubic equations of state (e.g., Peng-Robinson) for accurate gas behavior. For ANFIS, autoregressive/parallel configurations could capture spatiotemporal dependencies, while deep learning integration would handle complex datasets. Lastly, embedding bio-inspired algorithms (e.g., ant particle swarm optimization) into predictive control scheme. These enhancements aim to broaden the model's applicability to diverse separation systems, driving scalability and sustainability in the energy sector.

All the methodologies presented in this study will be applied to a N_2/O_2 separation process to optimize nitrogen injection in reservoirs. This injection is a key process, the main objective is for optimization and control in a hydrocarbon production system using ANNs and bioinspired system [18].

Acknowledgments

The first author thanks to CONAHCYT by its support via a scholar grant for Ph. D. studies. Likewise, the authors thank Universidad Autonoma del Carmen by allowing the facilities to develop this research project.

References

1. Chen, B., Dai, Y., Ruan, X., Xi, Y., & He, G. (2018). Integration of molecular dynamic simulation and free volume theory for modeling membrane VOC/gas separation. Frontiers of Chemical Science and Engineering, 12, 296-305. https://doi.org/10.1007/s1170 5-018-1701-3
2. Lu, H., Guo, L., Azimi, M., & Huang, K. (2019). Oil and Gas 4.0 era: A systematic review and outlook. Computers in Industry, 111, 68-90. https://doi.org/10.1016/j.compind.2019.06.007
3. Gbadamosi, A. O., Junin, R., Manan, M. A., Agi, A., & Yusuff, A. S. (2019). An overview of chemical enhanced oil recovery: recent advances and prospects. International Nano Letters. https://doi.org/10.1007/s40089-019-0272-8
4. Schwenzer, M., Ay, M., Bergs, T., & Abel, D. (2021). Review on model predictive control: An engineering perspective. The International Journal of Advanced Manufacturing Technology, 117(5-6), 1327-1349. https://doi.org/10.1007/s00170-021-07682-3

5. Ruz-Hernandez, J. A., Salazar-Mendoza, R., de la C, G. J., Garcia-Hernandez, R., & Shelomov, E. (2010). An approach based on neural networks for gas lift optimization. Soft Computing for Recognition Based on Biometric, Book Chapter, 207-224, Springer. https://doi.org/10.1007/978-3-642-15111-8_13
6. Castro-Peñaloza, Ulises., Pitalua-Diaz, Nun., Ruz-Hernández, José & Lagunas-Jiménez, Rubén. (2009). Introducción a los Sistemas Inteligentes. Universidad Autónoma de Baja California and Universidad de Sonora.
7. Ng, E. L. H., Lau, K. K., Lau, W. J., Ahmad, F., & others. (2021). Holistic review on the recent development in mathematical modelling and process simulation of hollow fiber membrane contactor for gas separation process. *Journal of Industrial and Engineering Chemistry.* https://doi.org/10.1016/j.jiec.2021.08.028.
8. Zendehboudi, S., Rezaei, N., & Lohi, A. (2018). Applications of hybrid models in chemical, petroleum, and energy systems: A systematic review. *Applied Energy, 228*, 2539–2566. https://doi.org/10.1016/j.apenergy.2018.06.051.
9. Asghari, M., Dashti, A., Rezakazemi, M., Jokar, E., & Halakoei, H. (2018). Application of neural networks in membrane separation. *Reviews in Chemical Engineering.* https://doi.org/10.1515/revce-2018-0011.
10. Cheng, X., Liao, Y., Lei, Z., Li, J., Fan, X., & Xiao, X. (2023). Multi-scale design of MOF-based membrane separation for CO2/CH4 mixture via integration of molecular simulation, machine learning, and process modeling and simulation. *Journal of Membrane Science, 672*, 121430. https://doi.org/10.1016/j.memsci.2023.121430.
11. Chu, Y., Lindbråthen, A., Lei, L., He, X., & Hillestad, M. (2019). Mathematical modeling and process parametric study of CO2 removal from natural gas by hollow fiber membranes. *Chemical Engineering Research and Design*, *148*, 45-55.
12. Medi, B., Vesali-Naseh, M., & Haddad-Hamedani, M. (2022). A generalized numerical framework for solving cocurrent and counter-current membrane models for gas separation. *Heliyon*, *8*(3).
13. Khalilpour, R., Abbas, A., Lai, Z., & Pinnau, I. (2013). Analysis of hollow fibre membrane systems for multicomponent gas separation. *Chemical Engineering Research and Design*, *91*(2), 332-347.
14. Chen, B., Ruan, X., Xiao, W., Jiang, X., & He, G. (2015). Synergy of CO2 removal and light hydrocarbon recovery from oil-field associated gas by dual-membrane process. *Journal of Natural Gas Science and Engineering*, *26*, 1254-1263.
15. Ruz-Hernandez, J. A., Matsumoto, Y., Arellano-Valmaña, F., Pitalúa-Díaz, N., Cabanillas-López, R. E., Abril-García, J. H., ... & Velázquez-Contreras, E. F. (2019). Meteorological variables' influence on electric power generation for photovoltaic systems located at different geographical zones in Mexico. *applied sciences*, *9*(8), 1649.
16. Pitalúa-Díaz, N., Arellano-Valmaña, F., Ruz-Hernandez, J. A., Matsumoto, Y., Alazki, H., Herrera-López, E. J., ... & Velázquez-Contreras, E. F. (2019). An ANFIS-based modeling comparison study for photovoltaic power at different geographical places in Mexico. *Energies*, *12*(14), 2662.
17. Arellano-Valmaña, F., Ruz-Hernandez, j. A., & Pitalúa-díaz, n. (2019). Modelo predictivo inteligente para la generación de energía eléctrica en un sistema fotovoltaico Intelligent forecast model for electrical power generation in a photovoltaic system. *Revista de Ingeniería*, *3*(10), 22-29.
18. Garcia-Sigales, B. J., Ruz-Hernandez, J. A., Rullán-Lara, J.-L., Alanis, A. Y., Ruz Canul, M. A., & Salazar-Mendoza, R. (in press). An approach based on neural networks and bioinspired systems for oil production systems optimization. In *Springer-Verlag*. Presented at the World Automation Congress (WAC) 2024, Cancún, Mexico.